J|A|C|S
COMMUNICATIONS

Published on Web 03/13/2008

An ICT-Based Approach to Ratiometric Fluorescence Imaging of Hydrogen Peroxide Produced in Living Cells

Duangkhae Srikun, Evan W. Miller, Dylan W. Domaille, and Christopher J. Chang*

Department of Chemistry, University of California, Berkeley, California 94720

Received December 30, 2007; E-mail: chrischang@berkeley.edu

The chemistry of hydrogen peroxide (H_2O_2) in living systems is receiving increasing attention owing to its diverse contributions as a marker for oxidative stress and damage events associated with aging and disease,[1] as a second messenger for cellular signal transduction,[2−4] or as a killing agent generated by immune cells to combat microbial invasion.[5] A key step toward elucidating the complex biological roles of this reactive oxygen metabolite is the development of new methods to monitor dynamic changes in peroxide concentrations generated within localized regions of the cell, as spatial and temporal variations in cellular H_2O_2 flows can lead to dramatically different physiological or pathological consequences. Small-molecule reporters offer one approach to meet this need,[6] and indicators that give a turn-on emission increase in response to H_2O_2 have been reported and applied for the study of peroxide biology.[7−15]

Despite advances in the development of new synthetic reagents, a limitation of intensity-based probes is that variabilities in excitation and emission efficiency, sample environment, and probe distribution pose potential problems for use in quantitative measurements. In contrast, ratiometric probes provide the practical advantage of built-in corrections for such variabilities by allowing simultaneous detection of two signals resulting from reacted and unreacted forms of the probe in the same sample.[16] We now present the synthesis and application of Peroxy Lucifer 1 (PL1), a new type of ratiometric fluorescent reporter for imaging H_2O_2 produced in living systems. Owing to its dual emission readout, PL1 is capable of visualizing highly localized changes in H_2O_2 concentrations generated by live cells in response to phagocytic stimulation while retaining the ability to spatially monitor relative [H_2O_2] fluxes throughout the rest of the sample.

Our approach to ratiometric fluorescence detection of cellular H_2O_2 relies on controlling internal charge transfer (ICT) within a dye platform to promote a change in its emission color upon reaction with H_2O_2. Specifically, modulation of the electron-donating 4-amino donor on a 1,8-naphthalimide (e.g., Lucifer Yellow) affects both ICT and emission color, as making this substituent more electron-deficient results in ICT-induced blue shifts in emission maxima. We reasoned that modifying the 4-amino donor into a more electron-withdrawing carbamate group that could be specifically decaged by H_2O_2 back to the amine would provide a switch for ratiometric detection of H_2O_2, a strategy inspired by indicators for pH,[17] anions,[18] metal ions,[19,20] and sugars.[21] On the basis of this design, the synthesis of Peroxy Lucifer 1 (PL1) is shown in Scheme 1.

We assessed the spectroscopic properties of PL1 under physiological-like conditions (20 mM HEPES, pH 7.4). In the absence of H_2O_2, PL1 displays one major absorption band centered at 375 nm (ϵ = 9600 $M^{-1}cm^{-1}$) with a corresponding blue-colored fluorescence maximum at 475 nm (Φ = 0.38). The relative blue shift of these absorption and emission features compared to other Lucifer-type dyes is consistent with ICT involving the relatively

Scheme 1. Synthesis and Action of Peroxy Lucifer 1 (PL1)

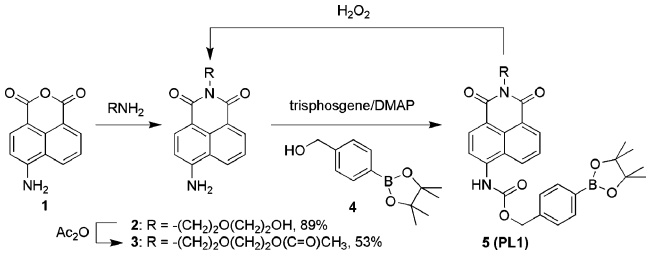

electron-poor carbamate donor. Reaction of PL1 with H_2O_2 triggers chemoselective cleavage of a boronate-based carbamate protecting group to deliver the green fluorescent aminonaphthalimide dye **3** as characterized by its absorption (λ_{abs} = 435 nm, ϵ = 8600 M^{-1} cm^{-1}) and emission (λ_{em} = 540 nm, Φ = 0.11) spectra, respectively (Figure 1a). The ratio of amine- to carbamate-derived emission intensities (F_{540}/F_{475}) upon excitation at 410 nm varies from 0.3 in the absence of H_2O_2 to 3.6 after complete conversion to **3**, a ca. 12-fold emission ratio change. Under pseudo-first-order conditions (1 μM PL1 and 1 mM H_2O_2), the observed rate constant for H_2O_2 deprotection is k_{obs} = 8.8 × 10^{-4} s^{-1}. The ratiometric emission response of PL1 is highly selective for H_2O_2 over other reactive oxygen species (Figure 1b). Compared to reactions with H_2O_2, the ratio of carbamate- to amine-substituted naphthalimides does not change appreciably with *tert*-butylhydroperoxide, hypochlorite,

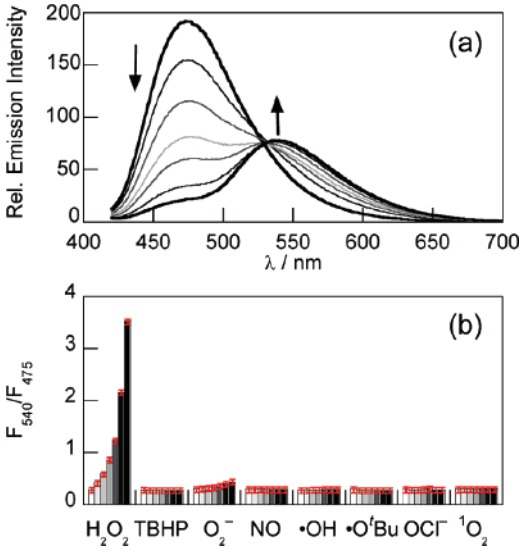

Figure 1. (a) Fluorescence response of 5 μM PL1 to 200 μM H_2O_2. Spectra were acquired before and 15, 30, 45, 60, 90, and 120 min after H_2O_2 was added. (b) Fluorescence responses of 5 μM PL1 to various reactive oxygen species (ROS) at 200 μM. Bars represent emission intensity ratios F_{540}/F_{475} at 0, 15, 30, 45, 60, 90, and 120 min after addition of each ROS. Data were acquired at 25 °C in 20 mM HEPES, pH 7.4, with excitation λ = 410 nm.

10.1021/ja711480f CCC: $40.75

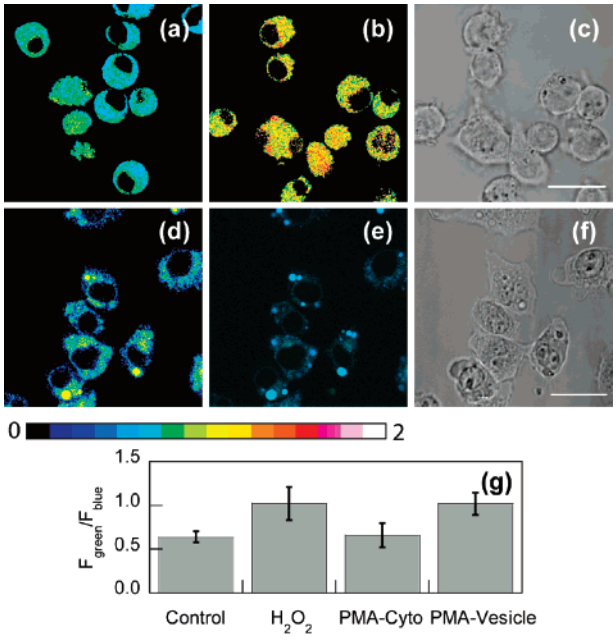

Figure 2. Confocal, ratiometric fluorescence images of live RAW 264.7 macrophage cells. Images displayed in pseudocolor represent the ratio of emission intensities collected in optical windows between 535−600 (green) and 430−495 nm (blue), respectively, upon two-photon excitation at 820 nm. (a) Cells incubated with 5 μM PL1 for 15 min at 37 °C. (b) PL1-loaded cells after treatment with 100 μM H_2O_2 for 60 min at 37 °C. (c) Brightfield images of cells in panel (b) with 20 μm scale bar. (d) PL1-loaded cells after treatment with PMA (1 μg/mL) for 30 min at 37 °C. (e) Cells in panel (d) showing only the green emission channel. (f) Brightfield image of cells in panels (d) and (e) with 20 μm scale bar. (g) Relative F_{green}/F_{blue} ratios displayed by cells loaded with PL1 only (control) and PL1-stained cells treated with H_2O_2 or PMA (cytoplasm vs vesicle).

superoxide, singlet oxygen, nitric oxide, hydroxyl radical, and *tert*-butoxy radical.

We next sought to apply PL1 for ratiometric fluorescence imaging of H_2O_2 in live biological samples. Two-photon confocal fluorescence images (820 nm excitation) taken of RAW 264.7 macrophages incubated with 5 μM PL1 indicate that the dye is cell-permeable (Figure 2a). The ratio image constructed from 535 to 600 nm (green) and from 430 to 495 nm (blue) fluorescence collection windows using ImageJ software gave an average emission ratio value of 0.6. Treatment of PL1-loaded cells with 100 μM H_2O_2 for 60 min triggers an increase in this ratio to ca. 1.0 (Figure 2b), consistent with H_2O_2-mediated boronate cleavage occurring within these cells. Macrophages incubated with PL1 only show negligible changes in emission ratio, and nuclear staining, flow cytometry, and trypan blue assays establish that the cells are viable throughout the imaging experiments (Figure S4). Experiments in HEK cells give similar results (Figure S3).

We then tested the ability of PL1 to detect endogenous bursts of H_2O_2 produced within living cells by stimulating PL1-loaded macrophages with phorbol myristate acetate (PMA) to induce phagocytosis-associated H_2O_2 generation.[22,23] The data in Figure 2d and e show clear increases in green-to-blue emission ratios localized within the phagocytic vesicles (>1.0) compared to other intracellular regions (0.6) upon PMA treatment, consistent with macrophage production of H_2O_2 to combat this insult. These data establish that PL1 is capable of live-cell imaging of H_2O_2 at natural immune response levels. Moreover, the ratiometric readout provided by this probe allows for detection of highly localized changes in H_2O_2 concentrations at phagocytic sites while at the same time visualizing [H_2O_2] variations throughout the rest of the cytoplasm.

In summary, we have presented the synthesis, properties, and live-cell evaluation of a new type of ratiometric fluorescent probe for H_2O_2. PL1 features a chemospecific H_2O_2 switch to modulate ICT with a marked blue-to-green emission color change. Experiments in macrophages show that PL1 can visualize H_2O_2 produced in living cells by ratiometric imaging. We are now using PL1 and related chemical tools to identify and quantify endogenous sources of biological H_2O_2, as well as expanding this general ICT design concept to detection of other important analytes in living systems.

Acknowledgment. We thank UC Berkeley, the Dreyfus, Beckman, Packard, and Sloan Foundations, the American Federation for Aging Research, and the National Institutes of Health (GM 79465) for funding. D.S. was supported by a scholarship from the Ministry of Science, Thailand. E.W.M. and D.W.D. thank the NIH Chemical Biology Graduate Program (T32 GM066698) and a Stauffer fellowship (to E.W.M.) for support. We thank Holly Aaron (UC Berkeley Molecular Imaging Center) for expert assistance, and Phung Gip for help with flow cytometry studies.

Supporting Information Available: Synthetic and experimental details. This material is available free of charge via the Internet at http://pubs.acs.org.

References

(1) Finkel, T.; Holbrook, N. J. *Nature* **2000**, *408*, 239−247.
(2) Rhee, S. G. *Science* **2006**, *312*, 1882−1883.
(3) Veal, E. A.; Day, A. M.; Morgan, B. A. *Mol. Cell* **2007**, *26*, 1−14.
(4) Giorgio, M.; Trinei, M.; Migliaccio, E.; Pelicci, P. G. *Nat. Rev. Mol. Cell Biol.* **2007**, *8*, 722−728.
(5) Miller, R. A.; Britigan, B. E. *Clin. Microbiol. Rev.* **1997**, *10*, 1−18.
(6) A protein-based fluorescent peroxide probe: Belousov, V. V.; Fradkov, A. F.; Lukyanov, K. A.; Staroverov, D. B.; Shakhbazov, K. S.; Terskikh, A. V.; Lukyanov, S. *Nat. Methods* **2006**, *3*, 281−286.
(7) Maeda, H.; Futkuyasu, Y.; Yoshida, S.; Fukuda, M.; Saeki, K.; Matsuno, H.; Yamauchi, Y.; Yoshida, K.; Hirata, K.; Miyamoto, K. *Angew. Chem., Int. Ed.* **2004**, *43*, 2389−2391.
(8) Xu, K.; Tang, B.; Huang, H.; Yang, G.; Chen, Z.; Li, P.; An, L. *Chem. Commun.* **2005**, 5974−5976.
(9) Lo, L.-C.; Chu, C.-Y. *Chem. Commun.* **2003**, 2728−2729.
(10) Onoda, M.; Uchiyama, S.; Endo, A.; Tokuyama, H.; Santa, T.; Imal, K. *Org. Lett.* **2003**, *5*, 1459−1461.
(11) Soh, N.; Sakawaki, O.; Makihara, K.; Odo, Y.; Fukaminato, T.; Kawai, T.; Irie, M.; Imato, T. *Bioorg. Med. Chem.* **2005**, *13*, 1131−1139.
(12) Wolfbeis, O. S.; Durkop, A.; Wu, M.; Lin, Z. H. *Angew. Chem., Int. Ed.* **2002**, *41*, 4495−4498.
(13) Chang, M. C. Y.; Pralle, A.; Isacoff, E. Y.; Chang, C. J. *J. Am. Chem. Soc.* **2004**, *126*, 15392−15393.
(14) Miller, E. W.; Albers, A. E.; Pralle, A.; Isacoff, E. Y.; Chang, C. J. *J. Am. Chem. Soc.* **2005**, *127*, 16652−16659.
(15) Miller, E. W.; Tulyathan, O.; Isacoff, E. Y.; Chang, C. J. *Nat. Chem. Biol.* **2007**, *3*, 263−267.
(16) Tsien, R. Y.; Poenie, M. *Trends Biochem. Sci.* **1986**, *11*, 450−455.
(17) Li, Z.-Z.; Niu, C.-G.; Zeng, G.-M.; Liu, Y.-G.; Gao, P.-F.; Huang, G.-H.; Mao, Y.-A. *Sens. Actuators B* **2006**, *114*, 308−315.
(18) Pfeffer, F. M.; Seter, M.; Lewcenko, N.; Barnett, N. W. *Tetrahedron Lett.* **2006**, *47*, 5241−5245.
(19) Liu, B.; Tian, H. *Chem. Commun.* **2005**, 3156−3158.
(20) Parkesh, R.; Lee, T. C.; Gunnlaugsson, T. *Org. Biomol. Chem.* **2007**, *5*, 310−317.
(21) Wang, J.; Jin, S.; Akay, S.; Wang, B. *Eur. J. Org. Chem.* **2007**, 2091−2099.
(22) Petty, H. R. *Biochim. Biophys. Acta* **1989**, *1012*, 284−290.
(23) Bellavite, P. *Free Radical Biol. Med.* **1988**, *4*, 225−261.

JA711480F